Development of Linear Irreversible Thermodynamic Model for Oxidation Reduction Potential in Environmental Microbial System

Hong-Bang Cheng, Mathava Kumar, and Jih-Gaw Lin*
*Institute of Environmental Engineering, National Chiao Tung University, Hsinchu City, Taiwan

ABSTRACT Nernst equation has been directly used to formulate the oxidation reduction potential (ORP) of reversible thermodynamic conditions but applied to irreversible conditions after several assumptions and/or modifications. However, the assumptions are sometimes inappropriate in the quantification of ORP in nonequilibrium system. We propose a linear nonequilibrium thermodynamic model, called microbial related reduction and oxidation reaction (MIRROR Model No. 1) for the interpretation of ORP in biological process. The ORP was related to the affinities of catabolism and anabolism. The energy expenditure of catabolism and anabolism was directly proportional to overpotential (η), straight coefficient of electrode (L_{EE}), and degree of coupling between catabolism and ORP electrode, respectively. Finally, the limitations of MIRROR Model No. 1 were discussed for expanding the applicability of the model.

INTRODUCTION

The pollution removal mechanisms in environmental bioengineering involves a number of oxidation reduction reactions, which are mediated by several kinds of microorganisms, including aerobic heterotrophs and autotrophs, facultative heterotrophs, and anaerobic heterotrophs (1). In such processes, the transfer of electrons between the oxidants and reductants convert the pollutants into harmless materials like carbon dioxide (CO_2) and water (H_2O). The electromotive force between the oxidants and reductants, defined as oxidation reduction potential (ORP) is used for the online quantification of the affinity of microbial reaction. The ORP measurement is sensitive and representative, therefore widely used to monitor (2,3) and control (4,5) the biological processes. Li and Bishop (5) correlated the measured ORP value to several other process parameters such as dissolved oxygen (DO), chemical oxygen demand (COD), and temperature during the nutrient removal process under different operating conditions of a wastewater treatment plant.

A typical reversible redox reaction is shown in Eq. 1 and the subsequent ORP in the solution can be represented by a generic Nernst equation as shown in Eq. 2.

$$c_1A_{red1} + c_2A_{oxi2} \rightleftharpoons c_3A_{oxi1} + c_4A_{red2} \quad (1)$$

$$E_e = E^0 - \frac{RT}{nF}\ln\frac{[a_{oxi1}]^{c_3}[a_{red2}]^{c_4}}{[a_{red1}]^{c_1}[a_{oxi2}]^{c_2}}, \quad (2)$$

where E_e is the equilibrium potential of the ORP electrode (V), E^0 is standard potential of ORP electrode for a given oxidation reduction process (V), R is gas constant (8.314 J K^{-1} mol^{-1}), T is absolute temperature (K), n is number of electrons transferred in the reaction, F is Faraday's constant (96,500 Coulomb mol^{-1}) and $[a]$ is activity of agent A. Under equilibrium condition, the ORP is correlated with oxidants and reductants using Nernst equation. The modified forms of Nernst equation used to control or interpret ORP value in biological processes (6–11) are listed in Table 1. The qualitative description of the relationship between ORP and ferric $[Fe^{2+}]$/ferrous $[Fe^{3+}]$ ions in the bacterial leaching process of chalcopyrite (6) is shown in Eq. 3. Janssen et al. (7) applied the linear relationship between ORP and sulfite to control the sulfate formation in the sulfite oxidizing process. The regression curves of ORP-sulfite diagrams were obtained by ion-selective electrode (ISE) (Eq. 4) and ORP platinum electrode combined with an Ag/AgCl reference electrode (Eq. 5). The slope of sulfate-ORP diagram obtained by ORP platinum electrode was in good agreement with the theoretically expected value (30.2 mV p^{-1} (HS^-) by Janssen et al. (7)), whereas, the value obtained by ISE was not closely matched with the theoretical value. This can only be described kinetically rather than thermodynamically (7) due to the limitation in the measurement of redox potential or electrode potential. Generally, redox potential measurement is limited by many factors, including electrode activeness of oxidants and reductants (12), and the surface properties of electrode (13). However, when ISE is used for the measurement, the effects of other ions can be diminished in the system (7). In addition, Pohland and Mancy (8) described the ORP measurement of methane synthesis process (Eq. 6) conducted with electrochemical indicator or mediator. Subsequently, Jones and Ingle (9) used immobilized redox indicator for the determination of sulfide reducing condition in synthetic solution. The degree of reduction of the indicator in contact with a given level of sulfide was modeled qualitatively by Eq. 7.

The ORP measurement for biological process is difficult to interpret by theoretical reasoning without the mediator addition or electrode modification with indicators (10). Nagpal et al. (10) investigated the ORP variation in sulfide reduction process theoretically as well as experimentally. However, the

Submitted December 21, 2006, and accepted for publication April 11, 2007.
Address reprint requests to Jih-Gaw Lin, Tel.: 886-3-5722681; Fax: 886-3-5725958; E-mail: jglin@mail.nctu.edu.tw.
Editor: Raimond L. Winslow.

0006-3495/07/08/787/08 $2.00
doi: 10.1529/biophysj.106.103507

TABLE 1 Modified Nernst equations and ORP models used for ORP data interpretation

Process	ORP Model		Reference
Bacterial leaching	$E_h = E_{mid} - \frac{RT}{F}\ln\frac{[Fe^{3+}]}{[Fe^{2+}]}$	(3)	Third et al. (6)
	E_h, the suspension redox potential. E_{mid}, standard redox potential under experimental conditions (i.e., at equimolar concentrations of Fe^{2+} and Fe^{3+} ion (0.695 V)) [Fe^{3+}] and [Fe^{2+}]: molar concentration of Fe^{2+} and Fe^{3+} ion (M)		
Sulfide oxidation	$E_t = -42 \cdot \log[HS^-] - 158$	(4)	Janssen et al. (7)
	E_t, measured redox potential at time t (mV) [HS^-], molar concentration of hydrogen sulfide (mg/L)		
	$E_t = -35 \cdot \log[HS^-] - 158$	(5)	
Methane biosythesis	$E_M = b - \frac{RT}{F}\ln[S]$	(6)	Pohland and Mancy (8)
	E_M, the equilibrium potential measured by indicator electrode. [S], molar concentration organic substrate b, constant		
Sulfate reducing	$E_{S/S^{2-}} = -0.475 - 0.0295\log[S^{2-}(aq)]$	(7)	Jones and Ingle (9)
	$E_{S/S^{2-}}$, redox potential of S^0(rhmb)/S^{2-} half-reaction at 25°C (mV) [S^{2-}(aq)], molar concentration of S^{2-} (aq) (μM)		
Sulfate reducing	$E[t] = 0.252 + 0.0075\log\frac{C_{SO_4^{2-}}}{C_{HS^-}} - 0.0657(-\log C_{H^+})$	(8)	Nagpal et al. (10)
	$E[t]$, ORP at time t (mV) $C_{SO_4^{2-}}$, C_{HS^-}, and C_{H^+}, concentration of SO_4^{2-}, HS^-, and H^+ (mg/L)		
Ferrous oxidation	$r = \frac{K_1 \times \exp\left[\frac{nF}{2RT}(E^m - Eh^0)\right] \times \left\{1 - \exp\left[\frac{-nF}{RT}(E^m - Eh)\right]\right\}}{1 + \frac{K_2}{[Fe^{2+}]} + K_3 \times \exp\left[\frac{nF}{RT}(Eh - Eh^0)\right]}$	(9)	Meruane et al. (11)
	r, The rate of electron transfer in reaction between Fe^{2+} and Fe^{3+} bound to the enzyme E^m, electrode potential measured Eh, the solution potential versus standard hydrogen electrode (V). Eh^0, the solution potential versus standard hydrogen electrode (V) of standard state. K_1, K_2, and K_3, kinetics constants [Fe^{3+}] and [Fe^{2+}], molar concentration of Fe^{2+} and Fe^{3+} ion (mg/L)		

theoretical value estimated by Nernst equation (Eq. 8) was high compared to experimental value. In biological pollution removal mechanism, microorganism utilizes negative entropy to resist the tendency of equilibrium and thus, entropy gradient results between the microorganisms and the external environment. Moreover, proton translocation exists between inner and outer parts of the cytoplasmic membrane, mediated by oxidation and reduction of substrate to induce ADP phosphorylation (14,15). Therefore, the microbial system undergoes irreversible equilibrium condition. Hence, the quantitative description of equilibrium by Nernst equation is inadequate to interpret the complex environmental biological process. However,

Nernst equation is used to predict ORP variation in nonequilibrium biological system with high approximation (16). To overcome the drawback, Meruane et al. (11) used electrode kinetics to describe the influence of solution potential (Eh) on the rate of Fe^{3+} ion oxidation by a nonequilibrium model (Eq. 9). However, the effects of electrochemical, heat, and ionic gradients on Fe^{3+} ion oxidation were not considered. From the above literatures, it is evident that more attention has to be made to overcome the drawbacks in the interpretation of ORP in nonequilibrium system. In this study, we focused on the development of an ORP model to describe the complex environmental microbial systems based on the principle of nonequilibrium thermodynamics.

Model development

The microbial ORP measurement system (Fig. 1 *a*) including bulk solution and thermal reservoir, is interconnected with the reactions and transport processes between the microbial energetic subsystem and ORP electrode subsystem. The overall system was developed based on the principle of electrochemistry and a constant volume of the system was assumed. The energy and material fluxes penetrating through the subsystems and their coupling are integrated for the development of new ORP model (Fig. 1 *b*). The microbial energy productive reaction proceeds far from equilibrium and therefore it is appropriate to describe the state of the system by thermodynamic variables. Galimov (17) examined the thermodynamic state of phosphorylation reaction by ^{13}C isotope and the interpretation revealed that biochemical systems are not necessarily far from equilibrium. Therefore, linear nonequilibrium thermodynamics (NET) could be applied to biological process (14,18,19). Hence, linear NET was used to describe the ORP measurement in the present microbial energetic subsystem.

Linear NET-based microbial energetic subsystem

The microbial energetic subsystem (S_M) includes cytoplasm (S_{CY}), bulk solution (S_{BS}), and thermal reservoir (S_{TR}) and the entropy variation in the subsystem is represented as in Eq. 10.

$$dS_M = dS_{BS} + dS_{CY} + dS_{TR}. \tag{10}$$

The rate of entropy production is changed by the synthetic activity of bacteria, however, it is zero under a steady state (20). As per second law of thermodynamics, entropy increases when a spontaneous or irreversible process, i.e., microbial process, approach equilibrium. To minimize the entropy increase in the system, microorganism requires minimum energy and it is generated due to the coupling of catabolism and phosphorylation in cytoplasmic membrane of prokaryotic cell (21–23). The energy released from adenosine triphosphate (ATP) is used to drive anabolism.

Anabolism is thermodynamically not spontaneous, because the reaction synthesizes new biomass and therefore decreases the entropy of the system. The catabolism and anabolism are combined macroscopically as an energetic coupling. Although several possible coupling modes of oxidation phosphorylation have been addressed (24), chemiosmotic hypothesis is more popular and hence it is used in this study. The variation of entropy in bulk solution is expressed as Eq. 11.

$$dS_{BS} = \frac{1}{T}dU_{BS} + \frac{P_{BS}}{T}dV_{BS} - \frac{\tilde{\mu}^{A}_{BS}}{T}dN^{A}_{BS} - \frac{\tilde{\mu}^{C}_{BS}}{T}dN^{C}_{BS} - \frac{\tilde{\mu}^{P}_{BS}}{T}dN^{P}_{BS} - \frac{\tilde{\mu}^{H}_{BS}}{T}dN^{H}_{BS}, \tag{11}$$

where U_{BS} (J), P_{BS} (N m^{-2}), and V_{BS} (m^3) are the internal energy, pressure, and volume of the bulk solution, respectively. $\tilde{\mu}^{A}_{BS}$, $\tilde{\mu}^{C}_{BS}$, $\tilde{\mu}^{P}_{BS}$, and $\tilde{\mu}^{H}_{BS}$(J mol^{-1}) are electrochemical potentials of anabolism, catabolism, oxidative phosphorylation, and proton translocation in bulk solution, respectively. N^{A}_{BS}, N^{C}_{BS}, N^{P}_{BS}, and N^{H}_{BS} are molecular numbers. The oxidation phosphorylation combined with electron transport system is coupled with the flux of catabolism, anabolism, and proton translocation in the cytoplasmic membrane as shown in Fig. 1 *b*. Usually, cytoplasm is relatively homogeneous mix of soluble proteins and other compounds. Hence, it is assumed that cytoplasm is in equilibrium and its entropy variation can be represented as Eq. 12.

$$dS_{CY} = \frac{1}{T}dU_{CY} + \frac{P_{CY}}{T}dV_{CY} - \frac{\tilde{\mu}^{A}_{CY}}{T}dN^{A}_{CY} - \frac{\tilde{\mu}^{C}_{CY}}{T}dN^{C}_{CY} - \frac{\tilde{\mu}^{P}_{CY}}{T}dN^{P}_{CY} - \frac{\tilde{\mu}^{H}_{CY}}{T}dN^{H}_{CY}, \tag{12}$$

where U_{CY}, P_{CY}, and V_{CY} are the internal energy, pressure, and volume of the cytoplasm, respectively. $\tilde{\mu}^{A}_{CY}$, $\tilde{\mu}^{C}_{CY}$, $\tilde{\mu}^{P}_{CY}$, and $\tilde{\mu}^{H}_{CY}$ are electrochemical potentials and N^{A}_{CY}, N^{C}_{CY}, N^{P}_{CY}, and N^{H}_{CY} are molecular numbers in cytoplasm. To eliminate the effect of temperature fluctuation, many researchers kept their bioreactors at a fixed temperature (i.e., steady state) by immersed in a thermal reservoir, for example, water bath. The variation of entropy in the thermal reservoir is represented as Eq. 13:

$$dS_{TR} = -\frac{1}{T}dU_{BS} - \frac{1}{T}dU_{CY}. \tag{13}$$

Total entropy of the microbial energetic system can be obtained by substituting Eqs. 11–13 into Eq. 10 and assuming the variation of the total system volume of components to be zero. Equation 10 can be rearranged as Eq. 14.

$$dS_M = -\left(\frac{\tilde{\mu}^{A}_{BS}}{T}dN^{A}_{BS} + \frac{\tilde{\mu}^{A}_{CY}}{T}dN^{A}_{CY}\right) - \left(\frac{\tilde{\mu}^{C}_{BS}}{T}dN^{C}_{BS} + \frac{\tilde{\mu}^{C}_{CY}}{T}dN^{C}_{CY}\right) - \left(\frac{\tilde{\mu}^{H}_{BS}}{T}dN^{H}_{BS} + \frac{\tilde{\mu}^{H}_{CY}}{T}dN^{H}_{CY}\right) - \left(\frac{\tilde{\mu}^{P}_{BS}}{T}dN^{P}_{BS} + \frac{\tilde{\mu}^{P}_{CY}}{T}dN^{P}_{CY}\right). \tag{14}$$

The rate of entropy production can be obtained as Eq. 15

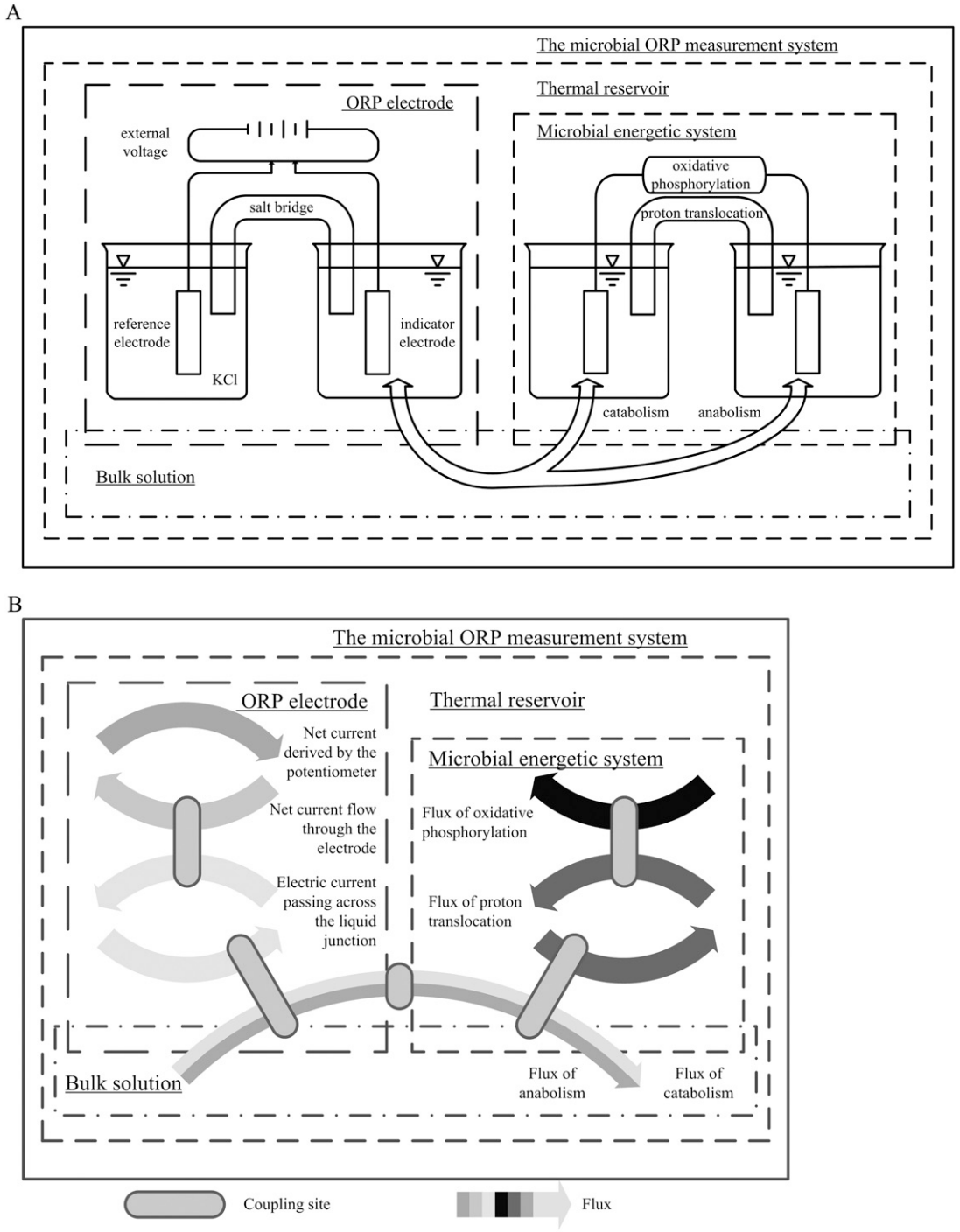

FIGURE 1 The framework of (*a*) energy and material fluxes transfer and (*b*) fluxes and their coupling in microbial ORP measurement system.

$$T\frac{dS_{\mathrm{M}}}{dt} = -\left(\tilde{\mu}^{\mathrm{A}}_{\mathrm{BS}}\dot{N}^{\mathrm{A}}_{\mathrm{BS}} + \tilde{\mu}^{\mathrm{A}}_{\mathrm{CY}}\dot{N}^{\mathrm{A}}_{\mathrm{CY}}\right) - \left(\tilde{\mu}^{\mathrm{C}}_{\mathrm{BS}}\dot{N}^{\mathrm{C}}_{\mathrm{BS}} + \tilde{\mu}^{\mathrm{C}}_{\mathrm{CY}}\dot{N}^{\mathrm{C}}_{\mathrm{CY}}\right) - \left(\tilde{\mu}^{\mathrm{H}}_{\mathrm{BS}}\dot{N}^{\mathrm{H}}_{\mathrm{BS}} + \tilde{\mu}^{\mathrm{H}}_{\mathrm{CY}}\dot{N}^{\mathrm{H}}_{\mathrm{CY}}\right) - \left(\tilde{\mu}^{\mathrm{P}}_{\mathrm{BS}}\dot{N}^{\mathrm{P}}_{\mathrm{BS}} + \tilde{\mu}^{\mathrm{P}}_{\mathrm{CY}}\dot{N}^{\mathrm{P}}_{\mathrm{CY}}\right), \tag{15}$$

where $\dot{N}$ is rate of change of molecular number. Assuming $\Delta\tilde{\mu}^{\mathrm{j}} = \tilde{\mu}^{\mathrm{j}}_{\mathrm{CY}} - \tilde{\mu}^{\mathrm{j}}_{\mathrm{BS}}$ (j equals to A, C, P, and H), Eq. 15 can be rewritten as Eq. 16.

$$T\frac{dS_{\mathrm{M}}}{dt} = -\left[\Delta\tilde{\mu}^{\mathrm{A}}\dot{N}^{\mathrm{A}}_{\mathrm{CY}} + \left(\dot{N}^{\mathrm{A}}_{\mathrm{CY}} + \dot{N}^{\mathrm{A}}_{\mathrm{BS}}\right)\tilde{\mu}^{\mathrm{A}}_{\mathrm{BS}}\right] - \left[\Delta\tilde{\mu}^{\mathrm{C}}\dot{N}^{\mathrm{C}}_{\mathrm{CY}} + \left(\dot{N}^{\mathrm{C}}_{\mathrm{CY}} + \dot{N}^{\mathrm{C}}_{\mathrm{BS}}\right)\tilde{\mu}^{\mathrm{C}}_{\mathrm{BS}}\right] - \left[\Delta\tilde{\mu}^{\mathrm{P}}\dot{N}^{\mathrm{P}}_{\mathrm{CY}} + \left(\dot{N}^{\mathrm{P}}_{\mathrm{CY}} + \dot{N}^{\mathrm{P}}_{\mathrm{BS}}\right)\tilde{\mu}^{\mathrm{P}}_{\mathrm{BS}}\right] - \left[\Delta\tilde{\mu}^{\mathrm{H}}\dot{N}^{\mathrm{H}}_{\mathrm{CY}} + \left(\dot{N}^{\mathrm{H}}_{\mathrm{CY}} + \dot{N}^{\mathrm{H}}_{\mathrm{BS}}\right)\tilde{\mu}^{\mathrm{H}}_{\mathrm{BS}}\right]. \tag{16}$$

Assuming the term $\left(\dot{N}^{\mathrm{j}}_{\mathrm{CY}} + \dot{N}^{\mathrm{j}}_{\mathrm{BS}}\right)$ equals to $\nu_{\mathrm{j}}J_{\mathrm{j}}$ (14), where, J_{j} is reaction rates of catabolism, anabolism, and oxidative phosphorylation with corresponding stoichiometric

coefficients, ν_j. The rate of change in molecular number of proton with respect to time between cytoplasm and bulk solution is zero. Hence, assuming $\left(\dot{N}^{H}_{CY}+\dot{N}^{H}_{BS}\right)$ is zero and the term $\nu_j\tilde{\mu}^{j}_{BS}$ as an affinity (A^{j}_{BS} in J mol^{-1}) (14), Eq. 17 can be obtained as follows.

$$T\frac{dS_M}{dt} = -\left[\Delta\tilde{\mu}^{A}\dot{N}^{A}_{CY} + J_A A^{A}_{BS}\right] - \left[\Delta\tilde{\mu}^{C}\dot{N}^{C}_{CY} + J_C A^{C}_{BS}\right] - \left[\Delta\tilde{\mu}^{P}\dot{N}^{P}_{CY} + J_P A^{P}_{BS}\right] - \left[\Delta\tilde{\mu}^{H}\dot{N}^{H}_{CY}\right]. \quad (17)$$

Under the condition of steady state, $\dot{N}^{j}_{CY}$ are zero for all $j \neq H$ and both $\Delta\tilde{\mu}^{H}$ and $-\dot{N}^{H}_{CY}$ are nonzero. This assumes $J_H = -\dot{N}^{H}_{CY}$ and Eq. 17 can be simplified according to the internal flux (14). Finally, Eq. 17 can be converged to Eq. 18.

$$T\frac{dS_M}{dt} = J_A A^{A}_{BS} + J_C A^{C}_{BS} + J_P A^{P}_{BS} + J_H\Delta\tilde{\mu}^{H}. \quad (18)$$

Combining microbial energetic and ORP electrode subsystems

The ORP variation is affected by catabolism as well as by anabolism in the biological system. In an ORP electrode subsystem, the fluxes of catabolism (J_C) and anabolism (J_A) transfer across the membrane of indicator electrode to the reference electrode (Ag/AgCl). The cell diagram of ORP electrode system can be represented as below (25).

$$\mathrm{Ag/AgCl/(c)KCl//sample/indicator\,electrode},$$

where [Ag/AgCl] is the internal reference element, [(c) KCl] is a reference solution compartment, and [//] is liquid junction. The composition of electrolyte in the indicator electrode is affected by J_C and J_A, and the potential difference mainly occurs at the interface (13). When the subsystem is viewed as an electrochemical cell, the ORP electrode subsystem shares the electrolyte with the microbial energetic subsystem, which results in the transfer of electrons from bulk solution to the electrode or vice versa. It was assumed in this study that oxidation reduction electrode can only transfer electrons and will not react with the sample in the bulk solution. In addition, the proton flux was ignored and the variation of proton concentration in bulk solution was mainly considered due to catabolism and anabolism. Also, the possibility of phosphorylation outside the microbial cell was excluded. Therefore, the total entropy variation of electrochemical cell of ORP electrode subsystem (S_{EL}) in Fig. 1 *a* can be represented as Eq. 19 (26,27).

$$T_{EL}\frac{dS_{EL}}{dt} = J(T_{EL}-T_{SU}) + \left(\tilde{\mu}^{A}_{EL}d\dot{N}^{A}_{EL} + \tilde{\mu}^{A}_{SU}d\dot{N}^{A}_{SU}\right) + \left(\tilde{\mu}^{C}_{EL}d\dot{N}^{C}_{EL} + \tilde{\mu}^{C}_{SU}d\dot{N}^{C}_{SU}\right) + i\eta + IE_j, \quad (19)$$

where T_{EL} and T_{SU} are the temperatures inside and surface of the ORP electrode system, respectively, i is the net current flow through the electrode, and η is overpotential (V). I is electric current passing across the liquid junction and E_j (V) is liquid junction potential. The temperature gradient between ORP electrode system and bulk solution was ignored because of the presence of thermal reservoir. Considering, the assumptions made to rewrite Eq. 16, the second and third terms of Eq. 19 can be rewritten as $-[\Delta\tilde{\mu}^{j}\dot{N}^{j}_{EL} + (\dot{N}^{j}_{EL}+\dot{N}^{j}_{SU})\tilde{\mu}^{j}_{SU}]$ (when $j = A$ and C). The composition of reference solution (i.e., KCl) is stable with respect to the characteristic time of internal processes of the ORP electrode (25). Hence, a steady state was assumed for the ORP electrode and therefore, the rate of change of molecular number in the ORP electrode ($\dot{N}^{j}_{EL}$, $j = A$ and C) was zero. In addition, complete mixing of the bulk solution was hypothesized. Therefore, the rate of change of molecular number ($\dot{N}^{j}_{SU}$) and electrochemical potential ($\tilde{\mu}^{j}_{SU}$) (when $j = A$ and C) on the surface of ORP electrode system are close to the rate of change of molecular number ($\dot{N}^{j}_{BS}$) and electrochemical potential ($\tilde{\mu}^{j}_{BS}$) of bulk solution, respectively. Consequently, Eq. 19 can be simplified to Eq. 20.

$$T_{EL}\frac{dS_{EL}}{dt} = -J_A A^{A}_{BS} - J_C A^{C}_{BS} + i\eta + IE_j. \quad (20)$$

Because liquid junction potential is stabilized by an outflow of the internal reference solution, the effect of liquid junction potential can be ignored. Therefore, Eq. 20 can be further simplified as Eq. 21.

$$T_{EL}\frac{dS_{EL}}{dt} = -J_A A^{A}_{BS} - J_C A^{C}_{BS} + i\eta. \quad (21)$$

The affinity of catabolism and anabolism in bulk solution induced the overpotential between the reference and indicator electrodes in Eq. 21. The mathematical relationship between overpotential and the variation of entropy is represented as the third term of Eq. 21. Overpotential (η) is defined as the electrode potential difference between equilibrium (E_e) and nonequilibrium (E_{ne}) conditions and it is related to current density by the Butler-Volmer equation based on mesoscopic nonequilibrium thermodynamics (28). The fluxes and forces in Eq. 21 are related in terms of phenomenological equations and hence, the fluxes can be written as a linear function of the forces as shown in Eqs. 22–24.

$$i = L_{EC}A^{C}_{BS} + L_{EA}A^{A}_{BS} + L_{EE}\eta \quad (22)$$

$$J_C = L_{CC}A^{C}_{BS} + L_{CA}A^{A}_{BS} + L_{CE}\eta \quad (23)$$

$$J_A = L_{AC}A^{C}_{BS} + L_{AA}A^{A}_{BS} + L_{AE}\eta. \quad (24)$$

An electrochemical cell represents true electromotive force (emf) when it produces no current, and operates in a reversible condition. The null point potentiometric method usually measures the emf of a cell as a multiple of standard emf generated by a stable reference cell. The emf supplied by potentiometer can be adjusted until it exactly equals the emf of the test cell and the emf supplied by the potentiometer is measured by an instrument using a standard cell of known emf (29). Therefore, ORP electrode system is operated under the condition of static head (19,30), the Eq. 22 can be rewritten as Eq. 25.

$$\eta = E_{ne} - E_e = P_{EC} A^{C}_{BS} + P_{EA} A^{A}_{BS}, \quad (25)$$

where $P_{EC} = (L_{EC}/L_{EE})$ and $P_{EA} = (L_{EA}/L_{EE})$.

Inserting Eq. 25 in Eqs. 23 and 24 gives Eqs. 26 and 27.

$$J_C = P_{CC} A^{C}_{BS} + P_{CA} A^{A}_{BS} \quad (26)$$

$$J_A = P_{AC} A^{C}_{BS} + P_{AA} A^{A}_{BS}, \quad (27)$$

where

$$P_{CC} = \left(L_{CC} - \frac{L_{CE}L_{EC}}{L_{EE}}\right), \quad P_{CA} = \left(L_{CA} - \frac{L_{CE}L_{EA}}{L_{EE}}\right),$$

$$P_{AC} = \left(L_{AC} - \frac{L_{AE}L_{EC}}{L_{EE}}\right), \quad \text{and} \quad P_{AA} = \left(L_{AA} - \frac{L_{AE}L_{EA}}{L_{EE}}\right).$$

The dissipation function (Eq. 21) can never be negative, hence, all straight coefficients, L_{ii} ($i = E$, C, and A) are positive. The relationship of P_{CA} in Eq. 26, and P_{AC} in Eq. 27 can be deduced according to Onsager reciprocal relations (27) as shown in Eq. 28.

$$\left(L_{CA} - \frac{L_{CE}L_{EA}}{L_{EE}}\right) = P_{CA} = \left(L_{AC} - \frac{L_{EC}L_{AE}}{L_{EE}}\right) = P_{AC}. \quad (28)$$

However, an inequality for phenomenological coefficients $\left(L_{ii}L_{jj} \geq L^2_{ij}\right)$ is also valid for all process in Eqs. 25–27, and $L_{ij} = L_{ji}$ (27). Hence, Eq. 29 is obtained as follows.

$$P_{CC} = L_{CC} - \frac{L_{CE}L_{EC}}{L_{EE}} \geq 0 \quad \text{and} \quad P_{AA} = L_{AA} - \frac{L_{AE}L_{EA}}{L_{EE}} \geq 0. \quad (29)$$

The ensemble of Eqs. 25–27 is named as Microbiological Related Reduction and Oxidation Reaction (MIRROR) Model No. 1. Using this model, the variation of oxidation reduction potential and fluxes of catabolism and anabolism can be quantified in nonequilibrium as well as equilibrium conditions.

DISCUSSION

Straight coefficients used in the MIRROR Model No. 1 were significant to relate the flux of its own force, however, the cross-coefficients, L_{ij} ($i, j = E, C$ and A whereas $i \neq j$) used in the model relates an indirect dependence of a flux on the direct forces of some other flux. In MIRROR Model No. 1, the energy conversion between the couples of input and output flux-force pairs was described in terms of cross-coefficients. The efficacy of energy conversion between different processes is related to degree of coupling (31). Therefore, it is important to quantitatively describe the degree of coupling by phenomenological coefficients. The couplings of ORP electrode process with catabolism and anabolism and their corresponding energy conversion are discussed as follows.

Electrode-activeness of redox couples by degree of coupling

Several sequential processes occur before the reactants are detected by the ORP electrode. Initially, the redox couples of reduction and oxidation are transported to electrode surface and consequentially, the electron transfer occurs between reactants and electrode due to coupled homogeneous reactions. Generally, ORP is affected by several factors, including the properties of electrode surface and redox couple of the species. If the redox couple is electrode active (e.g., Fe^{2+}/Fe^{3+}), it will greatly contribute to the ORP, and vice versa (12). Although the electrochemical potential can represent the electrical work performed by different species in the electrochemical system, the electrode activeness of the redox couples was not directly assessed in MIRROR Model No. 1. The electrode activeness is related to the couplings of electrode process with catabolism (q_C) and anabolism (q_A) and it can be quantified by the concept of degree of coupling (14), as shown in Eqs. 30 and 31.

$$q_C = \frac{L_{EC}}{\sqrt{L_{EE}L_{CC}}} \quad (30)$$

$$q_A = \frac{L_{EA}}{\sqrt{L_{EE}L_{AA}}}. \quad (31)$$

Under the condition of static head, the energy expenditures of catabolism and anabolism can be calculated by Eq. 32 (32).

$$\left(J_i A^{i}_{BS}\right) = \eta^2 \times L_{EE} \times \left(\frac{1}{q^2_i} - 1\right) i = C \quad \text{and} \quad A. \quad (32)$$

From Eq. 32, it is clear that energy required is inversely proportional to degree of coupling and directly proportional to L_{EE}. The relationship between overpotential and energy requirement is shown in Fig. 2. Overpotential is directly connected to current by L_{EE} and when the absolute value of overpotential is high, more energy is required for catabolism and anabolism to expend.

Efficacy of ORP measurement for catabolism and anabolism

In MIRROR Model No. 1, the efficacy of couplings (ε_i) of catabolism and anabolism with ORP measurements are evaluated by the definition of Caplan and Essig (19) as shown in Eq. 33.

$$\varepsilon_i = \frac{-\eta}{J_i A^{i}_{BS}} i = C \quad \text{and} \quad A. \quad (33)$$

After combining Eqs. 32 and 33, the efficacy of force can be rewritten as Eq. 34.

$$\varepsilon_i = \frac{-\eta}{J_i A^{i}_{BS}} = \frac{-\eta}{\eta^2 \times L_{EE} \times \left(\frac{1}{q^2_i} - 1\right)} = \frac{-1}{\eta \times L_{EE} \times \left(\frac{1}{q^2_i} - 1\right)}. \quad (34)$$

The relationship between overpotential, efficacy of catabolism/anabolism, and L_{EE} is shown in Fig. 3. It can be seen from Fig. 3 that efficacy is increased rapidly when overpotential is

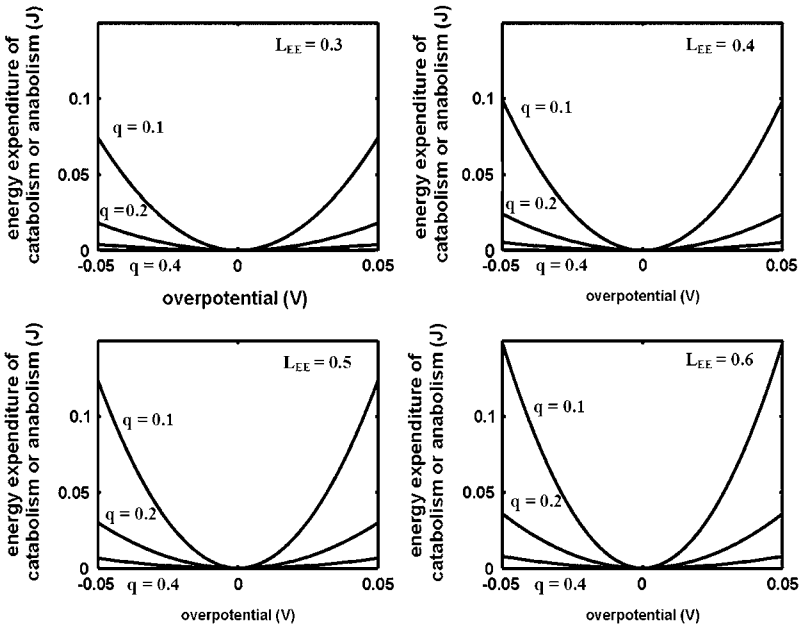

FIGURE 2 Variation of energy expenditure in microbial ORP measurement system under different overpotential, degree of coupling, q, and L_{EE} at static head.

close to zero and the corresponding results can be completely fitted using classical thermodynamics. However, overpotential will be zero only when all biochemical reactions are ignored and the corresponding biological system is under equilibrium condition.

At equilibrium condition both A_{BS}^{C} and A_{BS}^{A} are zero and therefore Eq. 25 can be rewritten as Eq. 35.

$$E_{ne} = \frac{L_{EC}}{L_{EE}} \times (0) + \frac{L_{EA}}{L_{EE}} \times (0) + E_e. \tag{35}$$

If Eqs. 2 and 35 are combined, which simplifies the MIRROR Model No. 1 into Nernst equation, as shown in Eq. 36.

$$E_{ne} = E_e = E^0 - \frac{RT}{nF} \ln \frac{[a_{oxi1}]^{c_3}[a_{red2}]^{c_4}}{[a_{red1}]^{c_1}[a_{oxi2}]^{c_2}}. \tag{36}$$

From Eq. 36, it is clear that MIRROR Model No. 1 can be extended to validate the ORP interpretation in nonequilibrium as well as equilibrium conditions, which is a unique feature compared to the other existing ORP models.

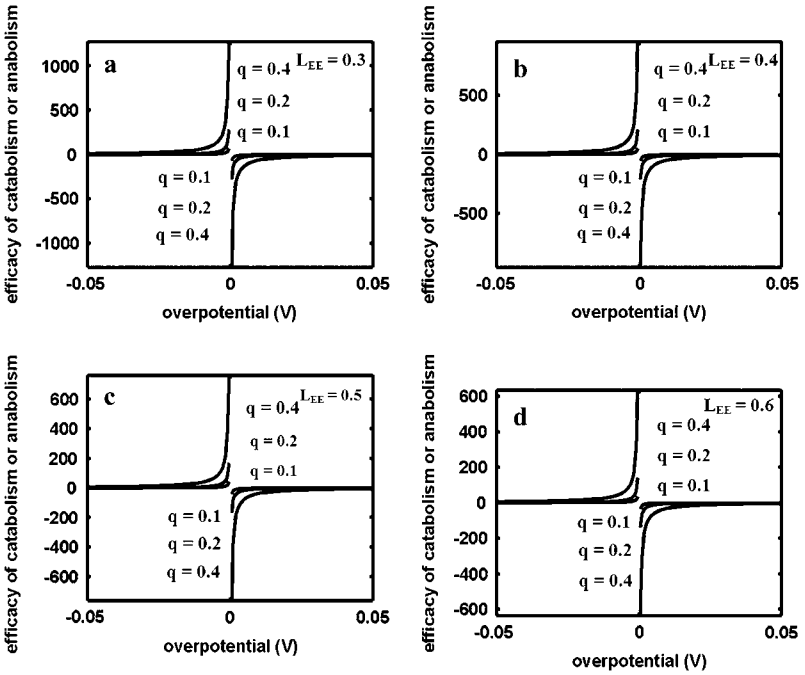

FIGURE 3 Variation of efficacies of catabolism and anabolism under different overpotential, degree of coupling, q, and L_{EE} at static head. $\tilde{\mu}$

CONCLUSIONS

In MIRROR Model No. 1, electrochemical potential, affinities, temperature, and overpotential gradients are combined based on the hypothesis of linear irreversible thermodynamics. The electrode activeness of redox couples was evaluated by phenomenological parameters of the model and the parameters that mainly affect the diagnosis of ORP data in the real situations is considered in the model development. Biomass was considered to produce from anabolism and affects the affinity of the reaction as well as the model structure. Therefore, to overcome this drawback, MIRROR Model No. 1 has to be investigated further.

We gratefully acknowledge financial support from the National Science Council, Taiwan, ROC (NSC 92-2622-E-009-021-CC3, NSC 94-2622-E-009-008-CC3).

REFERENCES

1. Tchobanoglous, G., F. Burton, and H. D. Stensel. 2003. Carbon and energy sources for microbial growth. *In* Wastewater Engineering: Treatment and Reuse. McGraw-Hill, London, UK. 563–565.
2. Balakireva, L. M., V. M. Kantere, and I. L. Rabotnova. 1974. The redox potential in microbiological media. *Biotechnol. Bioeng. Symp.* 4:769–780.
3. Tomlinson, J. W., and P. A. Kilmartin. 1997. Measurement of the redox potential of wine. *J. Appl. Electrochem.* 27:1125–1134.
4. Kjaergaard, L. 1977. The redox potential: its use and control in biotechnology. *In* Advances in Biochemical Engineering. T. K. Ghose, A. Fiechter, and N. Blakebrough, editors. Springer-Verlag, New York. 131–150.
5. Li, B., and P. Bishop. 2002. Oxidation-reduction potential (ORP) regulation of nutrient removal in activated sludge wastewater treatment plants. *Water Sci. Technol.* 46:35–38.
6. Third, K. A., R. Cord-Ruwisch, and H. R. Watling. 2002. Control of the redox potential by oxygen limitation improves bacterial leaching of chalcopyrite. *Biotechnol. Bioeng.* 78:433–441.
7. Janssen, A. J., S. Meijer, J. Bontsema, and G. Lettinga. 1998. Application of the redox potential for controlling a sulfide oxidizing bioreactor. *Biotechnol. Bioeng.* 60:147–155.
8. Pohland, F. G., and K. H. Mancy. 1969. Use of pH and pE measurements during methane biosynthesis. *Biotechnol. Bioeng.* 11:683–699.
9. Jones, B. D., and J. D. Ingle. 2005. Evaluation of redox indicators for determining sulfate-reducing and dechlorinating conditions. *Water Res.* 39:4343–4354.
10. Nagpal, S., S. Chuichulcherm, A. Livingston, and L. Peeva. 2000. Ethanol utilization by sulfate-reducing bacteria: an experimental and modeling study. *Biotechnol. Bioeng.* 70:533–543.
11. Meruane, G., C. Salhe, J. Wiertz, and T. Vargas. 2002. Novel electrochemical-enzymatic model which quantifies the effect of the solution Eh on the kinetics of ferrous iron oxidation with Acidithiobacillus ferrooxidans. *Biotechnol. Bioeng.* 80:280–288.
12. Peiffer, S., O. Klemm, K. Pecher, and R. Hollerung. 1992. Redox measurement in aqueous solutions: a theoretical approach to data interpretation, based on electrode kinetics. *J. Contam. Hydrol.* 10:1–18.
13. Yu, T. R., and G. L. Ji. 1993. Oxidation-reduction potential and its measurement. *In* Electrochemical Methods in Soil and Water Research. Pergamon Press, New York. 297–313.
14. Caplan, S. R., and A. Essig. 1969. Oxidative phosphorylation: thermodynamic criteria for the chemical and chemiosmotic hypotheses. *Proc. Natl. Acad. Sci. USA.* 64:211–218.
15. Jormakka, M., B. Byrne, and S. Iwata. 2003. Proton motive force generation by a redox loop mechanism. *FEBS Lett.* 545:25–30.
16. Morgan, J. J. 1967. Applications and limitations of chemical thermodynamics in natural water systems. *In* Equilibrium Concepts in Natural Water Systems. R. F. Gould, editor. American Chemical Society, Washington, DC. 1–29.
17. Galimov, E. M. 2004. Phenomenon of life: between equilibrium and nonlinearity. *Origins of Life and Evolution of Biospheres.* 34:599–613.
18. Caplan, S. R. 1968. Autonomic energy conversion. I. The input relation: phenomenological and mechanistic considerations. *Biophys. J.* 8:1146–1166.
19. Caplan, S. R., and A. Essig. 1983. Effectiveness of energy conversion. *In* Bioenergetics and Linear Nonequilibrium Thermodynamics. The Steady State. Harvard College Press, London, UK. 54–73.
20. Forrest, W. W., and D. J. Walker. 1964. Change in entropy during bacterial metabolism. *Nature.* 201:49–52.
21. Walz, D. 1979. Thermodynamics of oxidation-reduction reactions and its application to bioenergetics. *Biochim. Biophys. Acta.* 505:279–353.
22. Jin, Q., and C. M. Bethke. 2002. Kinetics of electron transfer through the respiratory chain. *Biophys. J.* 83:1797–1808.
23. Jin, Q., and C. M. Bethke. 2003. A new rate law describing microbial respiration. *Appl. Environ. Microbiol.* 69:2340–2348.
24. Caplan, S. R., and A. Essig. 1983. Energy coupling in mitochondria, chloroplasts, and halophilic bacteria. *In* Bioenergetics and Linear Nonequilibrium Thermodynamics. The Steady State. Harvard College Press, London, UK. 348–388.
25. Janata, J. 1989. Reference potential. *In* Principles of Chemical Sensors. Plenum Press, New York. 102–104.
26. Ratkje, S. K., and D. Bedeaux. 1996. The overpotential as a surface singularity described by nonequilibrium thermodynamics. *J. Electrochem. Soc.* 143:779–789.
27. McQuarrie, D. A., and J. D. Simon. 1999. Nonequilibrium thermodynamics. *In* Molecular Thermodynamics. University Science Books, Sausalito, CA. 581–627.
28. Rubi, J. M., and S. Kjelstrup. 2003. Mesoscopic nonequilibrium thermodynamics gives the same thermodynamic basis to Butler-Volmer and Nernst equations. *J. Phys. Chem. B.* 107:13471–13477.
29. Morris, J. G. 1974. Potentiometric measurement of electromotive force. *In* A Biologist's Physical Chemistry. Edward Arnold, London, UK. 331–332.
30. Hostettler, J. D. 1984. Electrode electrons, aqueous electrons, and redox potentials in natural waters. *Am. J. Sci.* 284:734–759.
31. Westerhoff, H. V., J. S. Lolkema, R. Otto, and K. J. Hellingwerf. 1982. Thermodynamics of growth. Non-equilibrium thermodynamics of bacterial growth. The phenomenological and the mosaic approach. *Biochim. Biophys. Acta.* 683:181–220.
32. Kedem, O., and S. R. Caplan. 1965. Degree of coupling and its relation to efficiency of energy conversion. *Trans. Faraday Soc.* 61:1897–1911.